

## Preparation of Thin Films of Greigite, $\text{Fe}_3\text{S}_4$ , and Its Preferred Orientation on a Sodium Chloride Crystal

HIROMOTO NAKAZAWA, T. OSAKA, AND K. SAKAGUCHI

National Institute for Researches in Inorganic Materials,  
Sakura-mura, Ibaragi, Japan

### Abstract

Thin films of greigite,  $\text{Fe}_3\text{S}_4$  (isometric,  $Fd\bar{3}m$ ), were deposited on a  $\{001\}$  face of sodium chloride by flash evaporation of an  $\text{Fe}_3\text{S}_4$  source material. The films exhibit a mixture of three types of preferred orientation: (1)  $\{001\}_{gr} \parallel \{001\}_{NaCl}$  with  $\langle 110 \rangle_{gr} \parallel \langle 110 \rangle_{NaCl}$ ; (2)  $\{111\}_{gr} \parallel \{001\}_{NaCl}$  with one of the  $\langle 110 \rangle_{gr}$  directions parallel to a  $\langle 110 \rangle_{NaCl}$  direction within the substrate face; (3)  $\{211\}_{gr} \parallel \{001\}_{NaCl}$  with a direction  $\langle 110 \rangle_{gr}$  lying in the contact plane and coinciding with one of the  $\langle 110 \rangle_{gr}$  directions of the type 2 film. The cubic closest packing of the sulfur atoms in greigite is believed to control the observed epitaxy.

### Introduction

The usual technique of vacuum deposition was used by Nakazawa and Sakaguchi (1972) to synthesize greigite,  $\text{Fe}_3\text{S}_4$ . In the present investigation, the flash evaporation technique of vacuum deposition (Harris and Siegel, 1948; Tressler and Stubican, 1967) is applied to prepare thin films of greigite in random orientation on amorphous carbon substrates and in preferred orientation on sodium chloride substrates. The results of the orientation relationships between deposit and NaCl substrate seem to indicate that the epitaxial growth of greigite is dominated by the arrangement of its larger (sulfur) atoms.

### Experimental

The initial powder evaporant was prepared by the usual dry method. Mixtures of pure iron and sulfur corresponding to the chemical composition  $\text{Fe}_3\text{S}_4$  were sealed and evacuated in silica tubes after mechanical mixing, and then heated at  $650^\circ\text{C}$  for about a week. After opening the tubes, the samples were ground and kept in acetone to prevent oxidation.

Shown in Figure 1 are the arrangement of the vapor source and substrate for the flash evaporation of the powder samples. The vapor source (Fig. 1) consisted of an aluminum ribbon (a) on which rested a strip of fine powder (b). When the ribbon was rolled up at constant speed around a shaft (c), the powder fell into a tungsten helical basket heater (d) via a curved tantalum strip (e). Though the shaft was rotated manually, the average deposition rate of

samples was controllable and estimated by the time needed to drop all the weight of sample.

Plates (f) of sodium chloride,  $7 \times 7 \text{ mm}^2$ , cleaved on  $\{001\}$  in air, as well as similar plates coated by amorphous carbon, were pasted by silver paint on the lower surface of the aluminum plate (g). The temperature of the plate can be controlled by the nichrome heater (h) on the upper surface of the plate and separated by a mica film. A thermocouple (i) was connected by silver paint to one of the sodium chloride plates, which served as a dummy substrate, to measure the surface temperature. The accuracy of the surface temperature measured by this device was within the range of  $\pm 2^\circ\text{C}$ , as assessed by the melting point of lead. The distance between the substrate surface and the evaporation source was 160 mm for all experiments.

The entire apparatus was sealed and evacuated in a belljar. The vacuum before evaporation was consistently better than  $2 \times 10^{-6} \text{ mm Hg}$  and was determined by a Phillips gauge after baking the apparatus. The temperatures of the evaporation source, and of substrate surface during evaporation, were about  $1700^\circ\text{C}$  and  $150^\circ\text{C}$ , respectively. The deposition rates and the mean thicknesses of deposits were calculated from the mass of the evaporated sample and from the distance between the evaporation source and the substrate surface, radial evaporation from a point source being assumed.

After the sodium chloride substrate was dissolved in water, the thin films of greigite thereby released were mounted on a copper grid and examined by

transmission electron diffraction with an electron microscope (Hitachi, HU-11D).

## Results and Discussion

### Identification of the Deposits

A high resolution electron diffraction pattern was taken from the film deposited on {001} of a sodium chloride coated by carbon (Fig. 2). The mean thickness and the deposition rate of the film were 200 Å and 800 Å/min, respectively. The electron diffraction patterns of the several selected areas were also obtained. The diffraction patterns were always similar, indicating that the deposit was uniform over the film. The  $d$ -values of the reflections and their relative intensities are in good agreement with those of natural greigite,  $\text{Fe}_3\text{S}_4$ , as previously reported by Skinner, Erd, and Grimaldi (1964). Therefore, the film consisted of pure greigite and its composition did not deviate far from  $\text{Fe}_3\text{S}_4$  stoichiometry. Similar results were obtained for films with different mean thicknesses in the range 200 Å–800 Å formed at

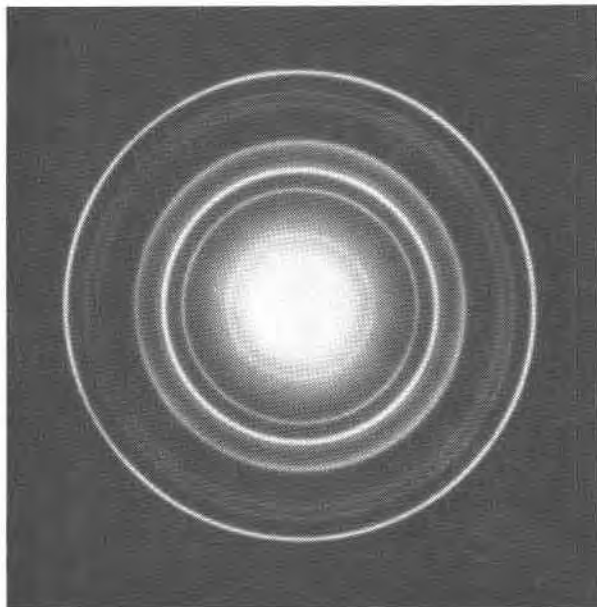


FIG. 2. High resolution electron diffraction pattern taken from the greigite film deposited on the (001) of a sodium chloride crystal coated by amorphous carbon.

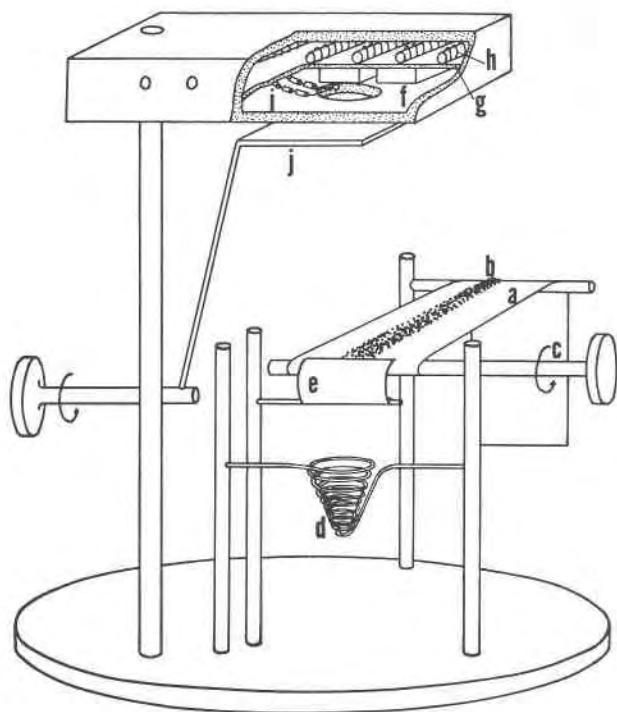


FIG. 1. The arrangements for the flash evaporation of powder samples with the  $\text{Fe}_3\text{S}_4$  composition. (a) aluminum ribbon, (b) powder evaporant, (c) shaft, (d) tungsten basket, (e) tantalum strip, (f) sodium chloride substrates, (g) aluminum plate, (h) substrate heater, (i) thermocouple, (j) shutter.

different deposition rates from 150 Å/min to 800 Å/min. In these experiments, the vacuum during evaporation was maintained at about  $4 \times 10^{-4}$  mm Hg.

The films deposited at very low deposition rates, for example, 100 Å/min or less, were contaminated by a new crystalline phase with an electron diffraction pattern which differed from that of any known iron sulfide. The amount of the unknown phase increased with decreasing deposition rate. The vacuum during the evaporation was not known in these experiments since it fluctuated widely between  $2 \times 10^{-6}$  to  $1 \times 10^{-4}$  mm Hg because of the irregular dropping of the powder into the heater. Study of chemical composition, crystal structure, and mechanism of formation of the unknown phase is now in progress. (Nakazawa, Osaka, and Sakaguchi, 1973).

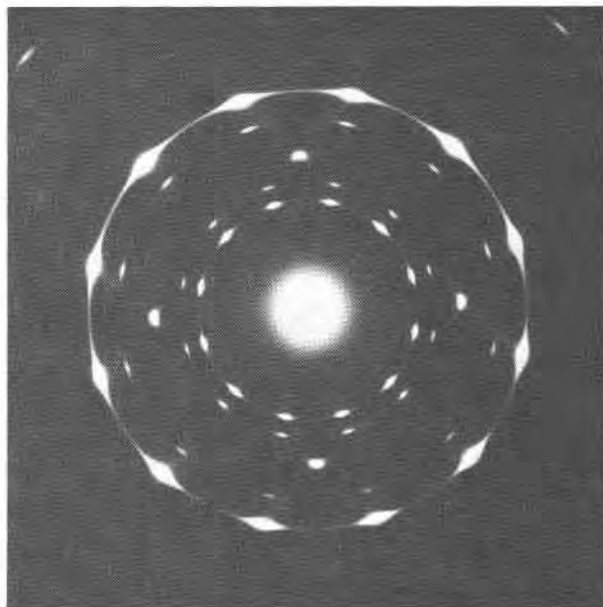
### Orientation of the Films

The greigite films grown on {001} of the sodium chloride substrate always exhibited preferred orientations. In preparing a sample for the electron microscope, each greigite film was cut into a square with edges parallel to  $\langle 100 \rangle$  of the sodium chloride substrate. Thus, even after the substrate was dissolved, the  $\langle 100 \rangle_{\text{NaCl}}$  directions remained known (relative to the film). The preferred orientations observed are

shown in Figure 3, which represents a bird's eye view of a {001} face of sodium chloride on which the 17 different orientations of epitaxial growths (A to Q) are schematically drawn. The arrows extending from these schematic orientations indicate one or more of their <110> directions that lie in the {001} plane of the substrate.

*The three types of orientation*

These 17 orientations may be grouped into three types (1) The {001} orientation wherein, as represented by crystal A,  $\{001\}_{gr} \parallel \{001\}_{NaCl}$  and all  $\langle 100 \rangle_{gr}$  directions are parallel to all  $\langle 100 \rangle_{NaCl}$  directions. (2) The {111} orientations wherein, as represented by crystals B to E,  $\{111\}_{gr}$  is in contact with and thus parallel to  $\{001\}_{NaCl}$  and wherein *one* of the  $\langle 110 \rangle_{gr}$  directions within the contact plane is parallel to *one* of the  $\langle 110 \rangle_{NaCl}$  directions. To emphasize that crystals B to E each represents a different crystallographic orientation, we add their {111}



A.

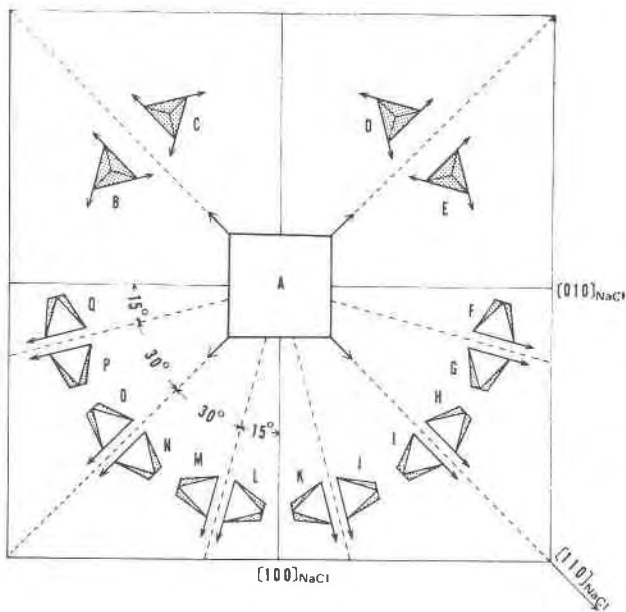
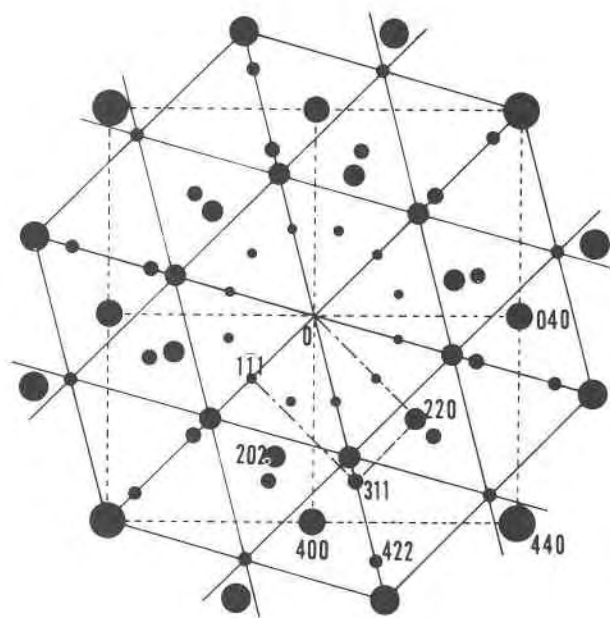


FIG. 3. Top view of the {001} surface of sodium chloride on which are schematically drawn the 17 different orientations (A to Q) observed for the epitaxial growths of greigite. For orientation A, the  $\{001\}_{NaCl}$  surface is in contact with  $\{001\}_{gr}$ . For symmetrically equivalent orientations B to E, the face in contact with  $\{001\}_{NaCl}$  is  $\{111\}_{gr}$ ; for F to Q, it is  $\{211\}_{gr}$ . Those  $\langle 110 \rangle$  directions of greigite that lie in the contact plane are drawn as arrows. No crystal forms could be resolved in the epitaxial deposits, but, for illustrative purposes, A is drawn as if its upper surfaces were bounded by cubic faces and B to Q are drawn as if their upper surfaces were bounded by {111} faces.



B.

FIG. 4. (A) High resolution electron diffraction pattern taken from the greigite film deposited on the (001) of a sodium chloride crystal cleaved in air. (B) Schematic illustration of the distribution of reflections. The superposition of the reciprocal net planes from the {111}, {001}, and {211} orientations are indicated by solid, broken, and long-short dashed lines, respectively.

planes that were not parallel to  $\{001\}_{\text{NaCl}}$  (shaded in Figure 3) even though such discrete planes were not actually observed. (3) The  $\{211\}$  orientation wherein  $\{211\}_{\text{gr}}$  is in contact with and thus parallel to the  $\{001\}_{\text{NaCl}}$  face of the substrate. Twelve distinct  $\{211\}$  orientations (F to Q in Fig. 3) are possible; again  $\{111\}$  planes have been added to crystals F to Q for illustrative purposes. For each crystal F to Q, the intersection between *one* or these added  $\{111\}$  planes and the  $\{211\}$  plane on which the crystal rests is a  $\langle 110 \rangle$  direction, shown by the arrow, that lies in the contact plane. Note that the arrow-indicated  $\langle 110 \rangle$  direction for orientations F and G is parallel to one of those for B and C. Similarly J and K have a  $\langle 110 \rangle$  direction in common with B and C. A characteristic of a  $\{211\}$  orientation is thus that it will have a  $\langle 110 \rangle$  direction within the contact plane which will be parallel to one of the  $\langle 110 \rangle$  directions for a  $\{111\}$  orientation.

Orientations of types 1 and 2 account for the strong reflections—for example, 200, 400, 440 and 220, 422 and 440—observed in the high resolution, electron-diffraction patterns of typical greigite films (Fig. 4A). To be more specific, the greigite reciprocal lattice is thus oriented as per the dashed lines in Figure 4B for the type 1 orientation but as per the solid lines for one of the type 2 orientations.

The remaining relatively weak reflections such as 111, 311, 222 and their equivalents are explained by the twelve different  $\{211\}$  orientations F to Q in Figure 3. The reciprocal lattice corresponding to one such orientation is indicated by long-short dashed lines in Figure 4b.

The  $\{211\}$  orientation in this investigation is explained by successive spinel-type twinning on  $\{111\}$  of greigite particles with the  $\{111\}$  and  $\{001\}$  orientations. The explanation is supported by the presence of diffuse streaks around 400 reflections in the electron diffraction pattern (Fig. 4a). The preferred orientations described above were not affected by change of deposition rate and film thickness in the range 150 Å/min–800 Å/min and 200 Å–800 Å, respectively.

The appearance of the  $\{111\}$ ,  $\{001\}$  and  $\{211\}$  orientations in the epitaxially grown particles of

greigite is similar to that in thin films of gold and other f.c.c. metals deposited onto a sodium chloride substrate (Ino, 1966; Mihama and Yasuda, 1966). This similarity suggests that the preferred orientation is due to some features which greigite and f.c.c. metals have in common. In the greigite crystal, with the spinel-type structure, small iron ions are in the interstices formed by the cubic close packing of large sulfur ions. It is, therefore, assumed that the arrangement of large ions has a dominant effect on the stabilities of the specific form and orientation of epitaxially grown particles.

Attempts to observe the crystal form of small particles of greigite by the bright field image in the electron microscope were, however, unsuccessful since the films 5–50 Å thick, formed by a low deposition rate of 5–100 Å/min, were contaminated by the unknown phase mentioned above.

### Acknowledgments

The authors are grateful to Professor N. Morimoto, Institute of Scientific and Industrial Research, Osaka University, for his encouragement and for improving the manuscript.

### References

- HARRIS, L., AND M. SIEGEL (1948) A method for the evaporation of alloys. *J. Appl. Phys.* **19**, 737–741.
- INO, S. (1966) Epitaxial growth of metals on rocksalt faces cleaved in vacuum. I. Orientation and structure of gold particles formed in ultrahigh vacuum. *J. Phys. Soc. Japan*, **21**, 346–362.
- MIHAMA, K., AND Y. YASUDA (1966) Initial stage of epitaxial growth of evaporated gold films on sodium chloride. *J. Phys. Soc. Japan*, **21**, 1166–1176.
- NAKAZAWA, H., AND K. SAKAGUCHI (1972) Anhydrous synthesis of greigite. *Mineral. J.* **6**, 458–463.
- , T. OSAKA, AND K. SAKAGUCHI (1973) A new cubic iron sulfide prepared by vacuum deposition. *Nature* (in press).
- SKINNER, B. J., R. C. ERD, AND F. S. GRIMALDI (1964) Greigite, the thio-spinel of iron; A new mineral. *Amer. Mineral.* **49**, 543–555.
- TRESSLER, R. E., AND V. S. STUBICAN (1967) Preparation of thin films of sulfospinel. *Mat. Res. Bull.* **2**, 1119–1124.

*Manuscript received, February 20, 1973; accepted for publication, May 2, 1973*